

Evidence of Distributed Interstitialcy-Like Relaxation of the Shear Modulus due to Structural Relaxation of Metallic Glasses

S. V. Khonik,¹ A. V. Granato,² D. M. Joncich,² A. Pompe,² and V. A. Khonik¹

¹*Department of General Physics, State Pedagogical University, 86 Lenin St., Voronezh 394043, Russia*

²*Department of Physics, University of Illinois at Urbana-Champaign, 1110 West Greet St., Urbana, Illinois 61801, USA*

(Received 4 May 2007; published 12 February 2008)

The interstitialcy theory is used to calculate the kinetics of shear modulus relaxation induced by structural relaxation of metallic glasses. A continuous distribution of activation energies is shown to be a salient feature of the relaxation. High precision *in situ* contactless electromagnetic acoustic-transformation shear modulus (600- kHz) measurements performed on a Zr-based bulk metallic glass are found to strongly support the approach under consideration. It is revealed that the activation energy spectra derived from isothermal and isochronal shear modulus measurements are in good agreement with each other. It is concluded that the increase of the shear modulus during structural relaxation can be understood as a decrease of the concentration of structural defects similar to dumbbell interstitials in simple crystalline metals.

DOI: [10.1103/PhysRevLett.100.065501](https://doi.org/10.1103/PhysRevLett.100.065501)

PACS numbers: 61.43.Fs, 62.20.de, 62.80.+f

In recent years, the general idea that basic thermodynamic and kinetic properties of supercooled liquids and glasses are governed by the unrelaxed (= high frequency) shear modulus G is gaining more and more acceptance. In particular, it was argued and experimentally confirmed that the activation energy of a viscous flow event in supercooled organic liquids is determined by the local G [1]. An excellent review of so-called elastic models for viscous flow of glass forming liquids utilizing a similar basic idea was recently given by Dyre [2]. Johnson and Samwer [3] proposed a universal law for inhomogeneous plastic flow of metallic glasses with G playing a central role. This role was also confirmed for homogenous flow of metallic glasses both below and above the glass transition temperature T_g [4,5]. Rather surprisingly, it was found that the ratio G/B (B is the bulk modulus) governs the ductile-brittle transition in metallic glasses [6]. Since B is rather insensitive to structural relaxation, it is the shear modulus that controls the embrittlement. An adequate understanding of the nature of shear modulus changes at different conditions turns out to be, therefore, a problem of major scientific and application importance.

Meanwhile, the unrelaxed shear modulus is the key physical quantity of the interstitialcy theory (IT) proposed by Granato [7]. This theory considers dumbbell interstitials (or similar defects in the case of complex materials; we nevertheless call them interstitialcies thereafter) to be the main structural defects of crystalline, liquid, and glassy states. It is shown below that the increase of G during structural relaxation of glass can be understood as a decrease of the concentration of interstitialcies.

The specific properties of interstitialcies—high shear susceptibility and large vibrational entropy—provide a comprehensive understanding of basic thermodynamic and kinetic properties of (supercooled) liquids and glasses within a common framework. In particular, the IT gives

quantitative explanations of some sound long-standing problems of condensed matter physics. Amongst these problems one can mention, first, the entropy of melting $\Delta S_m \approx 1.2k$ (per one particle, k is the Boltzmann constant) that holds all over the Periodic table with only a few exceptions [8]. This so-called Richard rule has remained unexplained since 1897, and the IT gives the exact ΔS_m -value [7,9]. The common interpretation of the known Lindemann melting rule (1910) implies that melting occurs when the vibration amplitude reaches a critical value A_c . Meanwhile, a fit to the experiment gives surprisingly small value for A_c , just only about 5% of the interatomic distance [8]. The IT analytically derives the Lindemann rule from a thermodynamic viewpoint with no connection to A_c giving the melting temperature proportional to the shear modulus [7] that is indeed observed [8]. The known decrease of G in the glass by 20–40% with respect to the crystal can be interpreted as the presence of 1–2% of interstitialcies, which effectively decrease G [9]. A decrease of the Debye temperature upon glass formation and its increase as a result of structural relaxation below T_g can be attributed to a change of the defect concentration, which controls G . The specific properties of quenched-in interstitialcies are supposed to define a number of heat capacity (C_p) and scattering effects. (i) Low temperature (5–10 K) Boson C_p -peak and corresponding peaks in neutron inelastic and Raman scattering are viewed within the IT as arising from low-frequency localized resonant vibration modes of interstitialcies [10]. The same resonant modes can be the source of the Einstein component in the total C_p , which was found in recent low temperature C_p studies (e.g., [11]). (ii) A decrease of C_p of liquids with temperature and C_p -change at $T = T_g$ can be explained within the IT as related to the fragility [9]. The fourth-order elastic constants of a metallic glass are in good agreement

with the predictions of the IT [12]. Finally, the well-known empirical Vogel-Fulcher-Tammann equation for the viscosity above T_g , which has remained unexplained so far, is analytically given by the IT in terms of the “fragility softness parameter” [13].

The IT also finds support in computer simulations. Indeed, Schober *et al.* [14,15] and others found small groups of atoms (10 atoms or more) that move collectively, in a “chainlike” (“stringlike”) fashion while neighboring atoms remain almost unaffected. Meanwhile, the stringlike low-frequency resonant vibration mode is just the basic dynamic feature of the interstitialcy configuration, which embraces movement of 10–20 atoms [16,17]. The existence of chain (string) motions was detected in simulations of different materials and prompted Oligschleger and Schober [15] to notice that such a behavior resembles the signature of interstitialcies in crystals. Recently, Nordlund *et al.* [18] found that the atoms in simulated liquid copper belonging to the chains (strings) have many of the same properties as interstitialcies in crystals, and the interstitialcies in glassy Cu have the expected properties of those in crystalline copper at high concentrations.

Recently, the IT was applied to derive the isothermal kinetics of structural relaxation and related shear modulus and viscosity behavior in glasses [19]. The analysis was performed using a single activation energy approach for defect activation during relaxation. It was later found that although this approach gives correct relaxation kinetics, the numerical values of the activation energy derived from real shear modulus data are unrealistic. The present Letter gives an analysis of the shear modulus relaxation for both isothermal and isochronal (=linear heating) conditions implying a distribution of activation energies. Specially performed *in situ* shear modulus measurements strongly support the obtained results.

As previously [19], we assume that a spontaneous decrease of the interstitialcy concentration during structural relaxation follows first-order kinetics. However, the corresponding activation energy E is supposed to be continuously distributed because of a distribution of local shear moduli due to fluctuations in local densities, chemical bonding, etc. Let $N(E, T, t)$ be temperature- and time-dependent defect concentration per unit activation energy interval. Then, the relaxation kinetics is given by $dN/N = -\nu \exp(-E/kT)dt$, where ν is the attempt frequency. If $N_0(E)$ is the initial interstitialcy concentration per unit activation energy interval (i.e., the initial activation energy spectrum, AES), then it is easy to show that after pre-annealing during time τ and subsequent annealing during time t , the interstitialcy concentration decreases to [20]

$$N(E, T, t) = N_0(E) \exp[-\nu(\tau + t) \exp(-E/kT)]. \quad (1)$$

The function $\Theta(E, T, t) = \exp[-\nu(\tau + t) \exp(-E/kT)]$ in Eq. (1) sharply increases near the “characteristic activation energy” $E_0 = kT \ln \nu(\tau + t)$ and to a good precision can be replaced by the Heaviside step function equal to 0 at

$E < E_0$ and 1 at $E > E_0$. The total concentration C of defects available for relaxation at a given instant is then given by integration over the AES:

$$C(T, t) = \int_{E_{\min}}^{E_{\max}} N(E, T, t) dE \approx \int_{kT \ln \nu(\tau + t)}^{E_{\max}} N_0(E) dE, \quad (2)$$

where E_{\min} and E_{\max} are the lower and upper limits of the AES available for activation and $N(E, T, t)$ is given by Eq. (1). Next, since only a small portion of the AES is scanned during an isothermal test, one can use the known “flat spectrum” approximation, $N_0 \approx \text{const} \neq N_0(E)$ [20]. Then, using the aforementioned step substitution for $\Theta(E, T, t)$, the concentration (2) is reduced to $C(t) = N_0 E_{\max} - N_0 kT \ln \nu(\tau + t)$. The basic equation of the IT gives an exponential decrease of the shear modulus with C , i.e., $G = G_x \exp(-\beta C)$, where β is a shear softening parameter and G_x is the shear modulus of the perfect crystal [7]. For defect copper, $\beta \approx 25$ defining a strong shear modulus softening with increasing C [7]. A similar value of β was recently determined for a bulk metallic glass [21]. For small C -changes, the modulus change $\Delta G(T, t)/G = -\beta \Delta C(T, t)$, where $\Delta C(T, t) = C_0 - C(T, t)$ is the change of the interstitialcy concentration. Supposing that G -measurement begins at $t = 0$ after pre-annealing during time τ and using the $C(T, t)$ -kinetics given above, the isothermal kinetics of the normalized G -change, $g(t) = G(t)/G_0 - 1$, becomes

$$g(t) = -\beta[C(t) - C_0] = \beta kT N_0 \ln(1 + t/\tau). \quad (3)$$

In the case of linear heating, the characteristic activation energy linearly increases with temperature, i.e., $E_0 = AT$, where $A \approx 3 \times 10^{-3}$ eV/K is weakly (logarithmically) dependent on the heating rate and attempt frequency [22]. Then, the isochronal modulus change is given by $g(T) = -\beta[C(T) - C_0]$ with $C(T) = \int_{AT}^{E_{\max}} N_0(E) dE$ and $C_0 = \int_{E_{\min}}^{E_{\max}} N_0(E) dE$. The last three formulae can be simply combined into

$$g(T) = \beta \int_{E_{\min}}^{AT} N_0(E) dE. \quad (4)$$

Equations (3) and (4) give the relaxation kinetics of the shear modulus upon isothermal and isochronal conditions, respectively. If $g(T)$ is converted into the dependence $g(E_0)$ using $E_0 = AT$, then Eq. (4) can be used for reconstruction of the initial AES, namely

$$N_0(E_0) = \beta^{-1} \partial g(E_0) / \partial E_0. \quad (5)$$

We performed a detailed check of the relaxation kinetics given by Eqs. (3) and (4) with the help of high precision *in situ* contactless shear modulus measurements carried out by an electromagnetic acoustic-transformation (EMAT) technique on bulk $\text{Zr}_{52.5}\text{Ti}_5\text{Cu}_{17.9}\text{Ni}_{14.6}\text{Al}_{10}$ (at.%) metallic glass. The initial glassy bars with the dimensions of $2 \times 5 \times 60$ mm³ were prepared by melt jet casting into a copper mold at a rate of $\approx 10^2$ K/s [23]. The glass tran-

sition temperature was found by differential scanning calorimetry to be ≈ 683 K at $dT/dt = 5.7$ K/min. X-ray checked bars were next cut into $2 \times 5 \times 8$ mm³ samples for EMAT measurements based on a method by Lyall and Cochran [24]. Frequency modulation and phase sensitive detection were used to continuously monitor the shear thickness vibration frequency $f \approx 600$ kHz of the sample. The relative precision of determination of the resonant frequency f was $\approx 10^{-5}$. The relative changes of f^2 were attributed to the relative changes of G . More experimental details are given elsewhere [25].

Both isothermal and isochronal runs were performed. In an isothermal run, the sample was heated at 5.7 K/min up to the testing temperature without overshooting, and subsequent automatic modulus measurements were carried out during a time interval ranging from 5 ks to (in a few cases) 400 ks. Temperature variations were kept within a few parts of a Kelvin. Nineteen runs in the temperature range $446 \leq T \leq 623$ K were performed. Isochronal runs were taken at 5.7 K/min up to 623 K.

A typical example of isothermal relaxation kinetics is shown in Fig. 1, which gives the time change of the normalized shear modulus $g = G/G_0 - 1 = f^2/f_0^2 - 1$ at $T = 509$ K during ≈ 85 ks. As is the case at all other temperatures, the shear modulus logarithmically increases with time after a transient of about a few kiloseconds. Although similar behavior is documented in the literature (e.g., [26]), it is to be emphasized that all ultrasound modulus studies known to us were actually carried out *ex situ* at room temperature after quenching the samples subjected to annealing treatments. Meanwhile, a correct analysis of the relaxation kinetics certainly requires *in situ* measurements as was done in the present Letter. Besides that, none of the known shear modulus measurements covers such long-time intervals.

We next checked whether the observed modulus kinetics follows Eq. (3). For this, a least-square fitting based on the Levenberg-Marquardt algorithm was applied allowing one to obtain the two unknown parameters, βN_0 and τ . It was found that Eq. (3) gives an excellent description of the

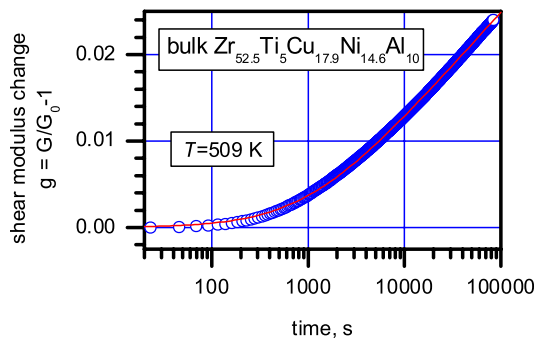


FIG. 1 (color online). An example of the relaxation kinetics of the change of the normalized shear modulus. After a transient of about a few ks, the shear modulus logarithmically increases with time. The solid curve give the least-square fit to Eq. (3).

relaxation in the whole time or temperature range investigated. In most of the cases, the reduced χ^2 -value is as low as $\approx 10^{-9}$ while the coefficient of determination $R^2 \approx 0.999$ and higher. It is to be also noted that Eq. (3) gives more complicated kinetics at short times as compared with the standard $\ln t$ -law in the usual AES approach [27]. The latter, besides that, does not provide any link between the defect and modulus relaxation.

Equation (3) allows a rough reconstruction of the AES as follows. An isothermal run scans a small portion of the AES corresponding to the energies ranging from $E_0^{\min} = kT \ln \nu \tau$ up to $E_0^{\max} = kT \ln \nu (\tau + t_{\max})$, where t_{\max} is the duration of a measurement run. Since Eq. (3) assumes a constant value of N_0 , the AES can be reconstructed as a set of horizontal segments corresponding to $N_0 = \text{const}$. This is shown in Fig. 2 for all testing temperatures, where the shear softening parameter β was accepted to be 25, the attempt frequency $\nu = 10^{13}$ s⁻¹, and τ was determined using the aforementioned fitting procedure. N_0 was calculated by two different ways: (i) using the same fitting procedure (open circles in Fig. 2) and (ii) from the long-time slope of $g(\ln t)$ -curves given by Eq. (3) as $\partial g / \partial \ln t = \beta k T N_0$ (closed circles in Fig. 2). Both methods give essentially the same result, and the defect concentration N_0 per unit activation energy interval rapidly increases with E_0 in the range 1.45 to 1.90 eV while a tendency of N_0 -decrease at higher E_0 is likely.

The AES represents a material parameter of glass. If reconstructed correctly, it has to be the same independently of the method used for data acquisition. In the case of isochronal tests, Eq. (5) can be used for AES reconstruction. To do this, the structural relaxation and anharmonic (linear in T) contributions to the total $g(T)$ -curve were separated according to $g(T) = g^{\text{sr}}(T) + g^{\text{anh}}(T)$. This is shown in Fig. 3, where open circles give the $g^{\text{sr}}(T)$ -component. After the latter dependence is converted to $g^{\text{sr}}(E_0)$, the AES can be calculated using Eq. (5) with $g = g^{\text{sr}}$. The result is given by open diamonds in Fig. 2. It is seen that AES reconstructions from independent isother-

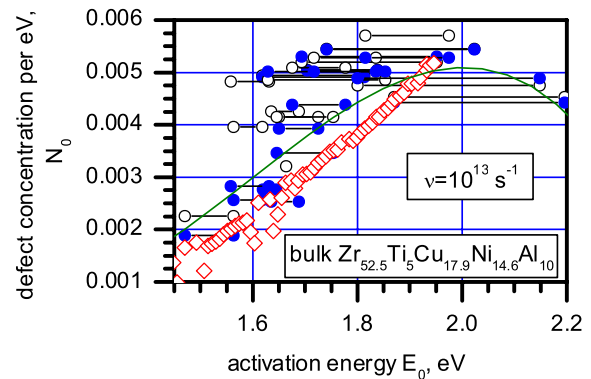


FIG. 2 (color online). Activation energy spectrum reconstructed from isothermal (horizontal segments) and isochronal (open diamonds) shear modulus measurements. The solid curve gives a polynomial approximation of the whole AES data set.

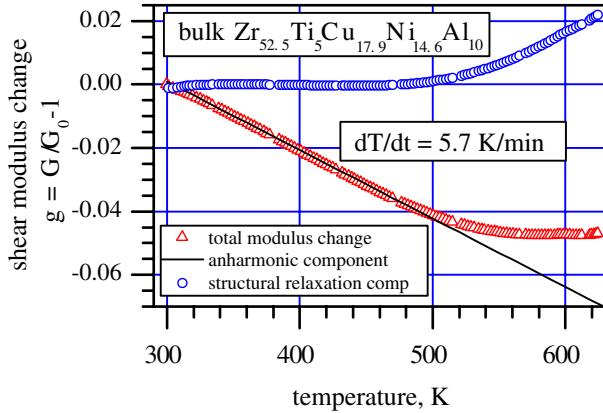


FIG. 3 (color online). Temperature dependence of the change of the normalized shear modulus at a heating rate of 5.7 K/min and its components due to anharmonicity and structural relaxation.

mal and isochronal G -measurements nicely agree with each other.

It is now possible to calculate the change of the interstitiality concentration ΔC due to structural relaxation in the temperature range investigated corresponding to activation energies $E_{\min} = 1.45 \lesssim E \lesssim E_{\max} = 2.2$ eV (Fig. 2). For this, we used the averaged AES, \bar{N}_0 , obtained by a third degree polynomial approximation (solid curve in Fig. 2). Then, $\Delta C = \int_{E_{\min}}^{E_{\max}} \bar{N}_0(E) dE \approx 0.003$. This is to be compared with the total interstitiality concentration in glass given by $C = \beta^{-1} \ln(G_x/G)$ [7]. The shear modulus of the glass under investigation in the as-cast state is $G \approx 0.6 \times G_x$ that gives the total initial concentration $C \approx 0.02$. Therefore, the defect concentration decreases by 15–20% in the course of annealing.

In conclusion, we calculated the kinetics of the shear modulus G within the interstitiality theory [7]. It is assumed that the decay of the concentration of basic structural defects—the entities similar to dumbbell interstitials—follows first-order kinetics with distributed activation energies. At $T = \text{const}$, G logarithmically increases with time after some transient according to Eq. (3). At $dT/dt = \text{const}$, the relaxation kinetics follows Eq. (4).

High precision *in situ* 600 kHz shear modulus measurements were used to test the obtained results. It was found that Eq. (3) gives a very accurate description of the relaxation kinetics and allows approximate reconstruction of the activation energy spectrum (AES) responsible for structural relaxation. The same AES was reconstructed from isochronal modulus measurements using Eq. (5). It was found that both spectra nicely agree with each other.

The results obtained provide the evidence that the G -increase upon structural relaxation can be understood as a decrease of the concentration of structural defects similar to dumbbell interstitials in simple crystalline met-

als. This concentration $C \approx 0.02$ in the initial glass decreasing by 15–20% in the course of annealing.

This work was supported by NSF No. DMR 01-38488.

- [1] J. C. Dyre, N. B. Olsen, and T. Christensen, *Phys. Rev. B* **53**, 2171 (1996).
- [2] J. C. Dyre, *Rev. Mod. Phys.* **78**, 953 (2006).
- [3] W. L. Johnson and K. Samwer, *Phys. Rev. Lett.* **95**, 195501 (2005).
- [4] W. L. Johnson, M. D. Demetriou, J. S. Harmon, M. L. Lind, and K. Samwer, *MRS Bull.* **32**, 644 (2007).
- [5] M. L. Lind, G. Duan, and W. L. Johnson, *Phys. Rev. Lett.* **97**, 015501 (2006).
- [6] J. J. Lewandowsky, W. H. Wang, and A. L. Greer, *Philos. Mag. Lett.* **85**, 77 (2005).
- [7] A. V. Granato, *Phys. Rev. Lett.* **68**, 974 (1992).
- [8] M. de Podesta, *Understanding the Properties of Matter* (Taylor & Francis, London and New York, 2002).
- [9] A. V. Granato, *J. Non-Cryst. Solids* **307–310**, 376 (2002).
- [10] A. V. Granato, *Physica B (Amsterdam)* **219–220**, 270 (1996).
- [11] Z. Zhou, C. Uher, D. Xu, W. L. Johnson, W. Gannon, and M. C. Aronson, *Appl. Phys. Lett.* **89**, 031924 (2006).
- [12] N. P. Kobelev, E. L. Kolyvanov, and V. A. Khonik, *Phys. Solid State* **49**, 1209 (2007).
- [13] A. V. Granato, *J. Non-Cryst. Solids* **352**, 4821 (2006).
- [14] H. R. Schober, C. Oligschleger, and B. B. Laird, *J. Non-Cryst. Solids* **156–158**, 965 (1993); H. R. Schober, *J. Phys. Condens. Matter* **16**, S2659 (2004).
- [15] C. Oligschleger and H. R. Schober, *Phys. Rev. B* **59**, 811 (1999).
- [16] P. H. Dederichs, C. Lehman, H. R. Schober, A. Scholz, and R. Zeller, *J. Nucl. Mater.* **69**, 176 (1978).
- [17] The atomic displacements connected with interstitiality formation and its vibration mode are shown in Refs. [9,13,18].
- [18] K. Nordlund, Y. Ashkenazy, R. S. Averback, and A. V. Granato, *Europhys. Lett.* **71**, 625 (2005).
- [19] A. V. Granato and V. A. Khonik, *Phys. Rev. Lett.* **93**, 155502 (2004).
- [20] V. A. Khonik, *Phys. Status Solidi A* **177**, 173 (2000).
- [21] U. Harms, O. Jin, and R. B. Schwarz, *J. Non-Cryst. Solids* **317**, 200 (2003).
- [22] V. A. Khonik, K. Kitagawa, and H. Morii, *J. Appl. Phys.* **87**, 8440 (2000).
- [23] A. E. Berlev, O. P. Bobrov, V. A. Khonik, K. Csach, A. Juríková, J. Miškuf, H. Neuhäuser, and M. Yu. Yazvitsky, *Phys. Rev. B* **68**, 132203 (2003).
- [24] K. R. Lyall and J. F. Cochran, *Can. J. Phys.* **49**, 1075 (1971).
- [25] C. A. Gordon, Ph.D. thesis, University of Illinois at Urbana-Champaign, Urbana, IL, 2000.
- [26] J. Filipecki and A. van den Beukel, *Scr. Metall.* **21**, 1111 (1987).
- [27] M. R. J. Gibbs, J. E. Evetts, and J. A. Leake, *J. Mater. Sci.* **18**, 278 (1983).